2. TECHNOLOGY DEVELOPMENT PROPOSAL

A. BACKGROUND

Imaging of intracellular calcium concentrations has assumed a central role in cellular physiology (Tsien, 1999). At the present time, calcium is usually imaged with synthetic fluorescent indicator dyes (e.g. fura-2, Oregon Green BAPTA-1, also known as OGB-1). Dyes have rapid kinetics and bright signals, but must be loaded into single cells by pipette or by bulk-loading of esterified indicator, which labels populations of cells with low contrast. More recently, a promising approach has arisen in the form of genetically encodable calcium indicators (GECIs; Tsien 2009, Looger and Griesbeck 2011). GECIs are engineered proteins that typically consist of (i) a calcium-sensing domain derived from calmodulin or troponin, (ii) a peptide domain that binds the calcium-sensing domain, and (iii) one or more XFP domains whose fluorescence intensities are modulated by the calcium-sensing interaction. Multicellular calcium imaging is of special interest in neuroscience, where systems-level function can be monitored only in intact circuitry. GECIs including GCaMP, cameleons, and TN-XXL have been used to image selected neuronal populations in flies, worms, fish, and mammals.

Despite recent advances in improving per-molecule signal (reviewed by Looger and Griesbeck 2011), GECI design is still beset by several challenges. The first is **dynamic range**. Conformational changes are driven by high binding cooperativity (n_H=3-4) so that fluorescence signals change over a narrow 3-5-fold range of calcium concentration, whereas synthetic indicators (n_H=1) have a 100-fold range. Many neurons fire throughout the <1 to 100 Hz range, including neocortical pyramidal neurons, interneurons, and cerebellar Purkinje cells. Currently, single GECIs are either poorly sensitive to single APs or do not give graded responses to firing rates above 10 Hz (Hendel et al. 2008). Calcium signals also drive synaptic plasticity and neurotransmitter release, with subsecond-to-second kinetics and a range of 0.1 – 10 μM (Yang, Tang, and Zucker 1999; Shouval, Wang, and Wittenberg 2010; Li et al. 2011), so that the ideal probe properties depend on the question at hand.

The second problem is **response kinetics**. BAPTA-based indicators have on-responses that are limited by diffusional processes (typical τ_{on} < 1 ms), and their signals terminate when calcium unbinds (for OGB-1, τ_{off} = 7 ms). Despite over a decade of development efforts, GECIs still typically have τ_{on} = 20 ms – 1.4 s and τ_{off} = 0.4 – 5 s (Hendel et al. 2008). Such slow kinetics degrade temporal resolution so that the true time course of calcium signals, and consequently spike times and variations in firing rate, cannot be accurately detected. GECI response times are limited by intramolecular probe dynamics. Thus monitoring neural activity will be aided tremendously by closing kinetic gaps in conformational GECI dynamics.

Innovation in the current proposal. A challenge in improving GECIs is to avoid de-optimization of existing beneficial features. In the case of Green fluorescent protein / Calmodulin protein sensor (GCaMP), such features include low degradation, high per-molecule brightness, and large fluorescence changes (Tian et al. 2009). We propose two innovations, using GCaMP3 as a starting scaffold. First, **we will engineer K_D** by making targeted changes that vary the affinity but preserve overall dynamics and probe kinetics. We will then co-express multiple variants at once with 1:1 stoichiometry. With co-expression of N probes of appropriate K_D, each variant will span ~1/N (in log units) of the total fluorescence range. Thus a **Virtual Negative Cooperativity (VNC)** effect (**Figure 1**) will be

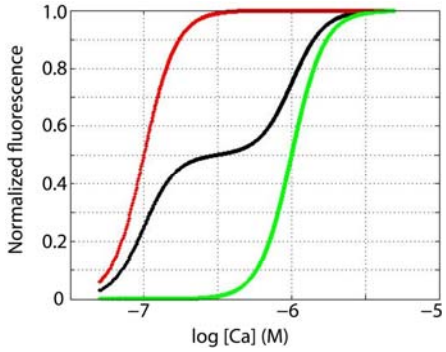

Figure 1. The Virtual Negative Cooperativity (VNC) concept. Co-expression of two GECIs of different affinity but equal brightness (red and green curves) will give a broader dynamic range (black). Variants of closer-spaced K_D or co-expressing a third variant would give a less inflected curve.

achieved in which each individual probe variant still has the same positive cooperativity, yet overall performance is spread over a wider range, as if n_H were decreased. Second, **we will engineer faster kinetics** to better track variations in calcium. Dendritic calcium signals can rise in 1 ms and fall in 10-100 ms (Higley and Sabatini 2008). By speeding indicator responsiveness, we will be able to track neuronal signaling events with unprecedented precision.

Approach. For VNC to work, GECIs must be developed with different K_D's, accelerated response speeds, and per-molecule brightness similar to one another. To reach these goals we are taking a structure-based design approach, which has already started to pay off. We already have varied-affinity and faster-kinetic versions of GCaMP3. Our eventual goal is to use these proteins for in vivo neurophysiology.

To change K_D, our approach is to replace residues whose side chains participate in calcium chelation, located in the EF-hands of calmodulin (**Figure 2;** Strynadka and James 1989; Procyshyn and Reid 1994; Wu and Reid 1997a,b; Black et al. 2000). EF-hand modification may also alter on- and off-rates of Ca binding by relieving bottlenecks in CaM conformational change. To alter GECI kinetics, our approach is to modify interactions between calmodulin (CaM) and RS20. The CaM-RS20 bound state is expected to trap calcium-bound calmodulin (Johnson et al. 1996), and response kinetics of GCaMP3 are slower than predicted from a single-step on/off-binding scheme. Disrupting CaM-RS20 interaction should speed fluorescence decay. Structure-function relationships for CaM and RS20 (Bagchi et al. 1992; Meador et al. 1992; Su et al. 1994; Chin and Means 1996; Chin et al. 1997) will be used to modify GCaMP3.

The two approaches above are innovative, but in other ways our strategy is conservative. We are not altering the fundamental design of GCaMP3, in the hope of retaining desirable features while reducing the risk of triggering new problems. For example, wholesale alteration of EF-hands to reduce cooperativity may render the probe nonfunctional by disrupting necessary calcium-dependent conformational changes. In the future we will revisit this challenge after we gain further insights into structure-function relationships.

Past research efforts that led to GCaMP3 involved screening hundreds of thousands of mutations (Tian et al. 2009), yielding improvements in proteolytic stability and per-molecule fluorescence. Such an exhaustive approach typically maximizes one parameter at a time, whereas kinetics have multiple parameters (K_D, off-responses, on-responses) that are potentially linked to one another. For example, a likely means of altering K_D is to manipulate interactions between CaM and its target, which then also affects on- and off-responses. Thus performance parameters are often linked in undesirable ways. Janelia Farm has sent us GCaMP5 variants for stopped-flow evaluation. They show little kinetic improvement.

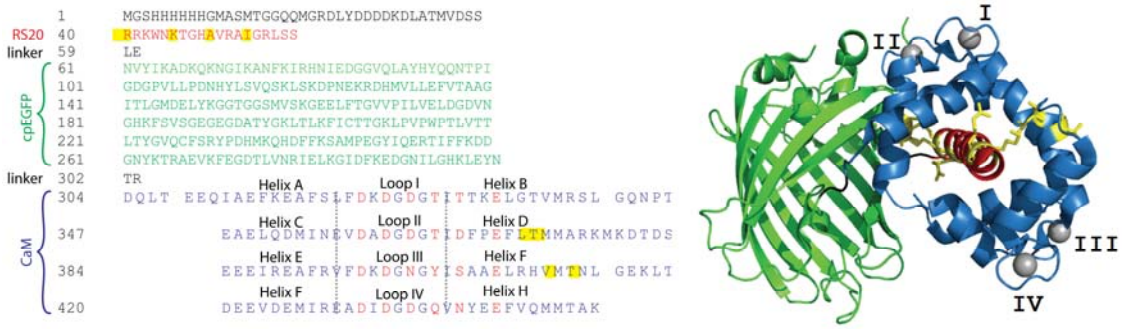

Figure 2. Sequence and calcium-bound structure of GCaMP3. *Left,* In the EF-hand domains of calmodulin (CaM), the loop I-IV calcium-chelating residues are indicated in red. These residues were mutated to generate the EF-series variants in this proposal. The yellow-highlighted residues in RS20 and CaM participate in calmodulin-RS20 contact and were mutated or deleted to generate the RS variants. *Right,* Calcium-bound structure of GCaMP3. Color coding matches the sequence. Yellow side chains indicate residues involved in CaM-RS20 contact. Calcium ions are indicated in gray.

B. SPECIFIC OBJECTIVES

OBJECTIVE 1: DEVELOP TOOLS FOR IMPROVED KINETICS AND DYNAMICS OF GCAMP IMAGING.

We will improve the kinetics and dynamics of GCaMP3 by engineering its calmodulin and calmodulin target domains to span a range of affinities and accelerate indicator responses to calcium. In preliminary work conceived and done entirely in my laboratory, we have demonstrated that both affinity and on-kinetics can be modulated by modifying acidic residues of calcium-binding EF-hands. We have accelerated off-kinetics by an order of magnitude or more by modifying a second target, the interface between calmodulin and its RS20 target, which we have discovered presents a kinetic bottleneck between calcium binding and fluorescence. We seek to build upon this progress by designing and testing optimal versions ("fast GCaMPs") that span at least one order of magnitude of K_D, as well as achieve 10-fold increases in signal on-kinetics and off-kinetics. We will furthermore develop vectors and methods to express and image fast GCaMPs in brain slices and in vivo. Combinations of indicators can sense an expanded concentration range than single indicators, an effect that we term Virtual Negative Cooperativity. We predict this strategy to be effective for GECIs whose K_D values differ by up to 40-fold, a range we have already attained.

OBJECTIVE 2: MONITOR NEURONAL CIRCUITS USING VIRTUAL NEGATIVE COOPERATIVITY GCAMP (VNC-CAMP).

Our long-term goal is to expand the concentration-sensitive range and temporal performance of GCaMP in intact brain tissue. In this Objective, our core strategy is to stoichiometrically express pairs of fast GCaMPs with different affinities in brain tissue, then image the combinations using two-photon microscopy. We will first validate the VNC-CaMP strategy in mammalian brain slices and in Drosophila neuromuscular junctions to calibrate fluorescence changes as a function of firing rates between <1 Hz and 100 Hz. Then, as proof of principle for in vivo physiology, we will use AAV-based viral vectors to express VNC-CaMPs in awake mice to monitor cerebellar activity changes during locomotion. These experiments will be done in three major neuron types: granule cells, molecular layer interneurons, and Purkinje cells. The availability of cell type-specific Drosophila driver lines, as well as cell- and tissue-specific Cre mouse lines from sources such as the Allen Institute for Brain Science and GENSAT, makes this Objective an important and timely contribution toward monitoring subcellular, single-cell, and circuit in intact brain tissue.

	Domain	K_d (μM)*	R_f	τ_{off} (ms)
Benchmarks				
OGB-1		0.24	14.0	7
GCaMP3		0.25	12.0	200
EF-hand Variants				
EF05	Loop III	0.16	6.8	180
L03	Loop IV	1.37	21.8	44
L03A	Loop IV	1.99	16.2	79
L05	Loop IV	3.39	12.3	30
L07b	Loop II	6.12	13.8	49
RS20 Variants				
RS06	CaM	0.31	6.5	41
RS05	CaM	0.47	8.5	34
RS08	CaM	0.63	10.0	29
RS09	CaM	0.69	9.5	31
RSd03	RS20	0.90	11.1	30
RSd05	RS20	1.19	10.7	16
RSd06	RS20	1.78	10.6	10
RSd09	RS20	3.81	4.1	4

*Measured at 25°C

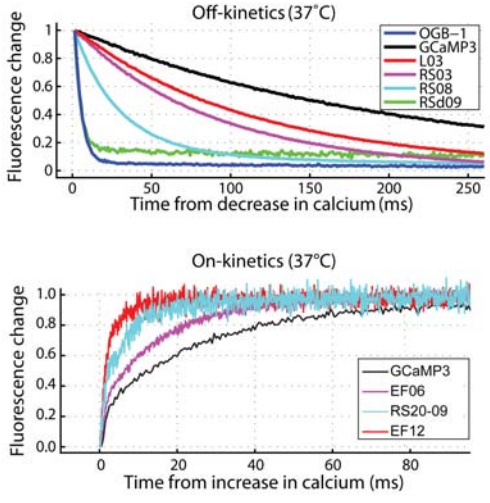

Figure 3. On- and off-kinetics of selected GCaMP variants at 37°C. Kinetic constants were determined on a stopped-flow fluorimetry apparatus using steps to >100 μM Ca^{++} and from 10 μM to 0 nM (τ_{off}). The black traces indicate GCaMP3.

C. PRELIMINARY RESULTS

GCaMP variants. GCaMP3 has slower kinetics than OGB-1 (**Figure 3**), indicating that its dynamics include bottlenecks imposed by probe conformational changes. A possible bottleneck is calmodulin's conformational response to calcium (Williams 1999; Faas et al. 2011); another is the association of calmodulin with RS20, the target region of myosin light chain kinase (Johnson et al. 1996; Nakai et al. 2001). Some promising variants are listed in **Figure 3**. We have attained a nearly 40-fold (0.16-6 μM) range of K_D without impairing per-molecule brightness. Of 55 variants we have made to date, 32 have acceptable dynamic range (R_f = F_{max}/F_{min} = 8-22; for GCaMP3, R_f=12). In an exciting development, in stopped-flow we have seen off-response times >10 times faster than other GECIs in wide use (**Figure 4;** Hendel et al. 2008). We generated most of these variants in the last six months, indicating a rapid pace of progress.

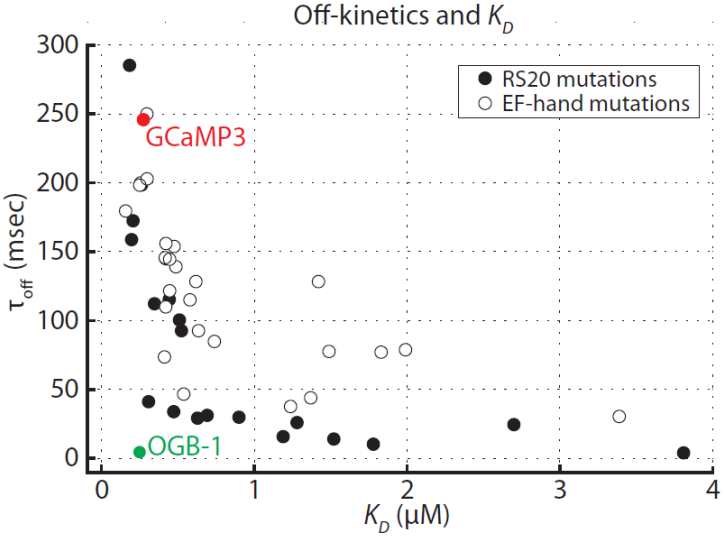

Figure 4 . Stopped-flow measurements at 37 °C of the off-response to a calcium step from 10 μM to 0 nM. Not shown are two additional GCaMP3 variants with K_D = 4-6 μM and τ_{off} = 20-50 ms.

EF-hand domain variants. Calmodulin (CaM; **Figure 2**, cyan) contains four EF-hand domains (Strynadka and James 1989) with up to six residues (underlined boldface) that participate in calcium chelation, forming the vertices of a coordination cage. The six residues form three acid pairs (X, Y, and Z) that strongly influence binding affinity (Reid and Hodges 1980; Procyshyn and Reid 1994; Wu and Reid 1997a,b). Our site-directed mutagenesis in loops I, II (Black et al. 2000), and III (Wu and Reid 1997b) has identified candidates for modulating binding affinity. The EF variant with the highest affinity (lowest K_D) is EF-05, which adds a Z acid-pair in loop III. Increased affinity is useful for detecting small signals evoked by single spikes. Variants with higher K_D will allow detection of calcium transients at higher firing rates. We have also neutralized calcium-chelating residues one loop at a time and found that X/Y/Z acidic residues in loops I and II are absolutely required for a working (high-R_f) probe.

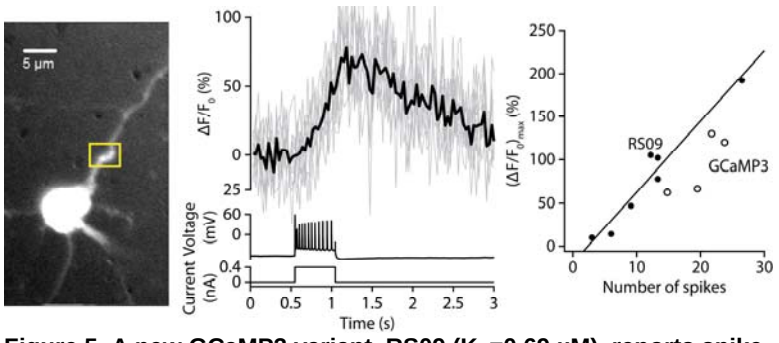

Figure 5. A new GCaMP3 variant, RS09 (K_D=0.69 μM), reports spike activity in neocortical neurons. *Left,* a layer 2/3 neuron recorded at room temperature (25°C) in neocortical slices from a P16 mouse after in utero electroporation at gestational day 15 (E15). *Center,* fluorescence change in RS09 in response to a 500-ms, 400-pA current injection to evoke an average of 13 action potentials (10 trials). *Right,* fluorescence change as a function of number of action potentials for various current steps. Open symbols show GCaMP3 responses under similar conditions.

RS20 domain variants. Calcium-bound CaM binds to the 19-amino acid RS20 domain (**Figure 2**), derived from smooth

muscle myosin light chain kinase. CaM rotates to form a hydrophobic channel that partially envelops RS20 (an alpha-helix) to produce maximal fluorescence. Based on known interaction residues (Bagchi et al. 1992; Su et al. 1994; Crivici and Ikura 1995; Chin and Means 1996) we have made several dozen variants by replacing CaM residues or replacing/deleting RS20 residues (**Figure 4**).

In cuvets, our variants have from 0.92 to 1.07 times the per-molecule brightness of GCaMP3. We have also tested variants in HEK cells, HeLa cells, and mouse neocortex, indicating that our approach is likely to yield usable variants. Testing in intact brain tissue, which is at an early stage, shows that variants respond to spike firing with similar fluorescence changes as GCaMP3 (**Figure 5**).

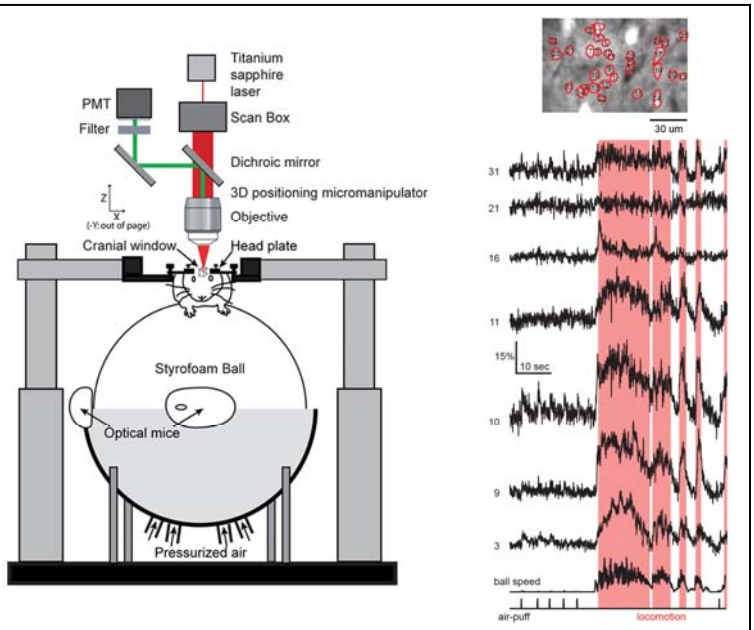

Figure 6, In vivo recording using GCaMP3 from cerebellar neurons in head-fixed mice. Left, head-fixed apparatus for imaging neural activity in awake locomoting mice (Dombeck et al. 2007). Right, granule cells expressing GCaMP3 in zone A of lobule IV/V of cerebellar vermis. Pink shading indicates locomotion.

In vivo imaging. GCaMP3 has been used to monitor hippocampal place cells (Dombeck et al. 2010) and cerebellar granule cells (Ozden et al. 2012). Our initial test beds for VNC-CaMP are neocortical brain slices, Drosophila neuromuscular junction, and cerebellar neurons in awake, behaving mice (Ozden et al. 2012).

We have injected mice with AAV-GCaMP3 in the cerebellar granule layer, then mounted the mice on a spherical treadmill for imaging. This is the first-ever calcium imaging of GCs in awake rodents. We have observed (**Figure 6**) locomotion-related signals in zone A of cerebellar lobule IV/V, representing trunk and hindlimbs. Rapid-rising signals (<200 ms) and falling signals with $t_{1/2}$ values in the range of 1-3 s are consistent with slow somatic calcium clearance and the slow off-kinetics of GCaMP3. Imaging of OGB-1/AM-loaded cells shows faster rise and fall times, suggesting that faster GCaMPs will give kinetic improvements.

D. Development Plan for the Proposed Technology

OBJECTIVE 1: DEVELOP TOOLS FOR IMPROVED KINETICS AND DYNAMICS OF GCAMP IMAGING

1.1 Improve the kinetics and vary the affinity of GCaMP3 variants. We have 17 variants that reduce τ_{off} to 50 ms or less at 37°C, a 4- to 50-fold improvement over GCaMP3. **Figure 4** shows that RS20 mutants often have significantly faster off-response than other GCaMP variants of comparable K_D. We have found that 9 out of 21 mutants tested to date have faster on-kinetics to large steps of calcium; of these, we characterized three in detail (**Figure 3**, lower right) and found that their on-kinetics are multiexponential and calcium-dependent. This complexity indicates the presence of energetic bottlenecks that are partially dependent on forward calcium binding. Since EF hand modifications affect calcium ion interactions and RS20 modifications affect the hydrophobic interface between CaM and RS20, combinations of the two types of

modification might retain the advantages of the individual modifications. This view is supported by the conformational arrangement of GCaMP3 determined crystallographically (Akerboom et al. 2009). EF+EF and RS20+RS20 combinations may also be favorable. We will generate combined mutants and use steady-state and stopped-flow fluorescence to identify variants with a range of affinities and the fastest combined on- and off-kinetics. We will search for variants with a range of K_D values from 0.2-2 μM, on-times of <2 ms for large calcium steps, and off-times of <20 ms, speeds that are within half an order of magnitude of Oregon Green BAPTA-1.

Alternate approaches and caveats: Because on-kinetics are complex and because the combined effects of mutations are often unpredictable, we will screen multiple variants in which on-responses are accelerated. Even if we find no promising combinations, our existing best variants can still be used to achieve a VNC effect.

1.2: DEVELOP REAGENTS FOR EXPRESSING AND IMAGING GCaMP VARIANTS IN MAMMALIAN BRAIN TISSUE. GCaMP variants passing the screening steps of Objective 1.1 will be expressed using in utero electroporation in neocortical layer 2/3 neurons and adeno-associated virus (AAV)-mediated delivery. To co-express GCaMP and mCherry with 1:1 stoichiometry, the sequences will be separated using a 2A peptide, which acts as a ribosomal skip mechanism (Donnelly et al. 2001) to generate two separate proteins. For electroporation, DNA constructs will be generated containing the CAG promoter (cytomegalovirus immediate-early enhancer element coupled with the chicken beta-actin promoter; Doll et al. 1996) and the enhancer element WPRE (woodchuck posttranslational regulatory element). The resulting construct, CAG-GCaMP variant-P2A-mCherry-WPRE, will when injected and electroporated into the embryonic brain drive expression in neocortical layer 2/3 pyramidal neurons (Mainen et al. 1999; Mao et al. 2008). For AAV delivery, plasmid (pAAV) constructs will be made, pAAV-SYN-GCaMP-P2A-mCherry-WPRE (SYN=synapsin promoter), for integration, packaging, and generation of high-titer AAV at the U. Penn. AAV Core Facility. Expressing neurons will be identified and characterized using two-photon imaging, as used in our previous work (Sullivan et al. 2005, Sarkisov and Wang 2008, Ozden et al. 2009, Granstedt et al. 2009, 2010).

1.2a. Test high-affinity GCaMP variants in brain slices for expression and detection of single action potentials. The fluorescence ratio of GCaMP and mCherry will be used to quantify probe brightness, including depolarization-evoked trains of action potentials to measure fluorescence signals (**Figure 5**). These measurements will be compared with the EGFP-mCherry ratio as a benchmark. Successful variants will have GCaMP brightness comparable to the brightness of the purified protein observed in Objective 1.1. Variants with significantly reduced brightness will not be pursued further.

Distinguishing individual spikes requires high affinity and improved off-response of GCaMP. We will express fast off-rate variants and make patch clamp recordings to obtain single-spike signals. Scans across the proximal dendrite and the axon initial segment will identify the fastest signals, which can be <100 ms (Higley and Sabatini 2008; Hires et al. 2009). For comparison with GCaMP3 and OGB-1 we will quantify single-spike $\Delta F/F$, rising $t_{1/2}$, and falling $t_{1/2}$. Because GCaMP and mCherry may be differentially degraded, the GCaMP-mCherry ratio will be measured 1 to 8 weeks after AAV injection to determine the useful lifetime of GCaMP.

1.2b. Test low-affinity GCaMP variants in brain slices for spike-rate detection. Lower-affinity variants are expected to show lower sensitivity to single spikes, but show steadily increasing fluorescence as a function of firing rate. Layer 2/3 neurons expressing such variants will be depolarized to fire at 1-100 Hz. Transient and steady-state measurements will be made to determine a transfer function for calcium signal as a function of firing rate. Particular attention will be paid to the falling time course, which may be altered at high calcium concentrations (Higley and Sabatini 2008). An upper limit to the measurable firing rate will be determined on a neuron-by-neuron basis, and the statistics used to place a bound on in vivo performance. Based

on results with GCaMP and other high-affinity probes (Mao et al. 2008; Hendel et al. 2008), proximal dendritic calcium is an increasing function of firing rate up to 30-60 Hz.

Alternate approaches and caveats: Further across-the-board improvement will require modification of the GFP core. Although all preliminary work reported in this application was done solely in my laboratory, I am aware of efforts to improve probe brightness at Janelia Farm, where I have a collaboration planned. Their Next Generation GECI project is a medium-throughput facility (available as a service) that screens hundreds of variants per year using 96-well neuronal culture and in vivo fly and mouse assays. In their own work they have targeted single-spike $\Delta F/F$ as a parameter for improvement. Many of their improvements come from changes in linker domains and domains enclosing the GFP chromophore, and are orthogonal to our EF-hand and RS20 domain changes. This suggests that our mutations may be combined with their variants; in one preliminary result we have found that combining GCaMP5 with RS09 leads to a 3-fold decrease in τ_{off}.

Another contingency is the possibility that signals will vary among cells at high firing rates (i.e. >30 Hz) because of variation in the amount of calcium entry, clearance, or buffering (endogenous or from GCaMP itself). If this variation is very high, Objective 2 will be refocused on observing firing rates below 30 Hz, and large signals will be interpreted in terms of relative rather than absolute firing rate.

Long-term prospects. If time permits after completion of Objective 1, we have an exploratory strategy for improving on-kinetics. Very large calcium steps (**Figure 7**) reveal a ~1 ms rising response (see also Nakai et al. 2001 Fig. 3D inset), considerably faster than the 10-80 ms rise times reported for GCaMP3 in vivo. Millisecond responses would be useful for detecting signals in calbindin-positive neurons, which potentially outcompete GCaMP3. We suspect that binding of calcium to CaM loops III and IV is a rate-limiting bottleneck for modest-sized signals since they bind calcium first, before loops I and II (Weinstein and Mehler 1994). We have found that X/Y/Z neutralization of loop III or IV leaves GCaMP3 functional, but neutralizing loop I or II reduces R_f to ~2. To emphasize the ~1 ms response, speculative strategies include (a) locking loops III and IV in a bound-like conformation using acid-base pairing or disulfide bonds, (b) replacing them with sequences resembling calpain, which has n_H=2 and no loop III/IV binding, and (c) enhancing the calcium-binding affinities of loop I and II.

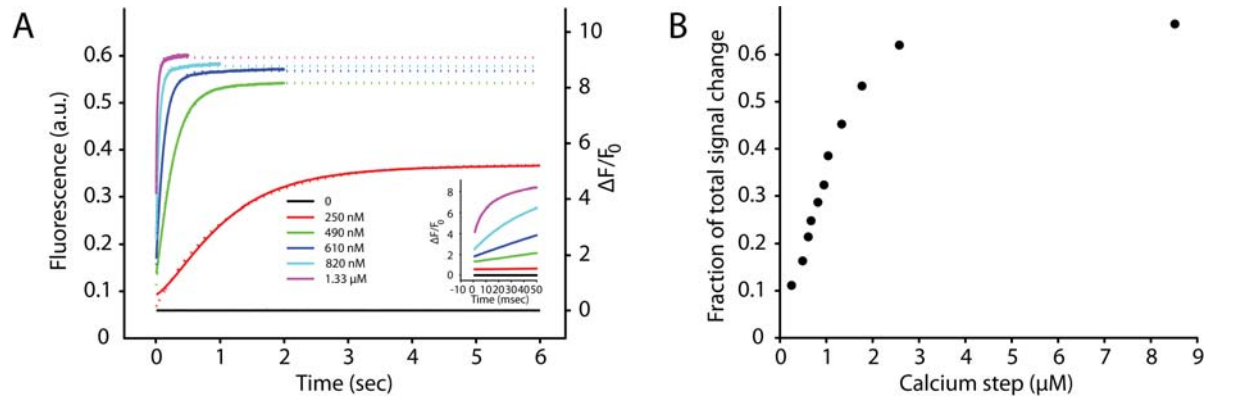

Figure 7: Millisecond on-response of GCaMP3 to a micromolar step in calcium. A, Fluorescence responses to increases in calcium from 0 nM to different concentrations, measured in purified GCaMP3 using stopped-flow kinetic apparatus. At concentrations above 500 nM (cyan and purple traces), a rapid jump becomes apparent that occurs within the dead time of the stopped flow, ~1.5 ms (see jumps at t=0 ms, inset). **B,** Fraction of the total change in fluorescence contained in the rapid jump, as a function of the calcium step size. The rapid jump is seen for most GCaMP variants generated to date, but not for the synthetic indicator Oregon Green BAPTA-1.

OBJECTIVE 2: MONITOR NEURONAL CIRCUITS USING VIRTUAL NEGATIVE COOPERATIVITY GCaMP (VNC-CaMP).

In this Objective we will use combinations of improved GCaMP3 variants to image function in brain slices, Drosophila neuromuscular junction, and awake, behaving mice. We will take advantage of the properties of VNC-CaMP to perform physiological measurements that would previously have been difficult without genetic targeting and/or improved GECIs. We will record neural activity from three major neuron types of the cerebellum during behavior to test ideas of function suggested by brain slice experiments. The applications here emphasize mammalian in vivo imaging, a principal interest of the laboratory. However, GECI imaging has broad applications in invertebrate and vertebrate cell physiology.

Achieving a VNC effect will require co-expression of two or more GECIs. For multiple GCaMP variants of high sequence homology, alternate codons will be used to eliminate recombination. The general approach will be to identify one fast-performing variant for a given range of K_D, then co-express variants of different K_D. To confirm that the construct makes both proteins, purified protein mixtures will be characterized using steady-state fluorimetry to estimate stoichiometry and determine the fluorescence vs. calcium function.

2.1 Spike readout in mammalian brain slices. We will combine the results of Objective 1.2a/b to achieve a VNC effect. As in Objective 1.2, we will make cell-attached or whole-cell patch clamp recordings while evoking small numbers of action potentials or action potential trains of various frequencies. Calcium signal $\Delta F/F$, rising $t_{1/2}$, and falling $t_{1/2}$ will be compared with the results from single fast GCaMPs and compared with the prediction that VNC-CaMP readout approximates the sum of the two separate functional relationships. Performance will be benchmarked against GCaMP3, GCaMP5, and OGB-1. VNC-CaMP performance will be quantified in the form of a $\Delta F/F$ vs. firing rate curve. The criterion for whether VNC has achieved improvements in dynamic range will be to measure the range of firing over which a 10%-90% signal range is reached. In addition, we will measure response speed and the signal-to-noise ratio occurring after a small number (1 to 5) of spikes.

2.2 Spike readout at Drosophila neuromuscular junctions. As a second test of the ability of our variants to report neural activity, we will express and image VNC-CaMP in Drosophila using the Gal4/UAS system (Brand and Perrimon, 1993). Promising variants will be cloned into cDNA constructs allowing UAS-controlled expression. Transgenic Drosophila lines will be generated through P-element-mediated germ-line transfection (Spradling and Rubin, 1982). Subsequently, the UAS-GECI lines will be crossed with Gal4 flies to produce offspring with cell-type specificity (e.g. elav^{C155}-Gal4 for pan-neuronal expression; Lin and Goodman, 1994). A standardized preparation for quantifying spike readout properties is the presynaptic bouton of the neuromuscular junction, which has fast calcium dynamics and is easily imaged (Hendel et al. 2008; Tian et al. 2009). For these experiments we will collaborate with Prof. Mala Murthy. Calcium signals will be quantified as in Objective 2.1.

Alternate approaches and caveats: Mammalian brain expression of two variants should be possible using in utero electoporation (IUE) or AAV. VNC-CaMP performance may deviate from the sum of individual curves if P2A-based coexpression is not stoichiometric, or if per-molecule F_{max} is unequal. Deviation will be compensated by measuring combined calcium-dependence of purified protein and by measuring dependence of fluorescence on firing rate in neuron culture. For three variants, near AAV's maximum capacity of ~4.5 kb, pseudorabies virus (PRV) may be used (Granstedt et al. 2008, 2009).

A future priority is the use of VNC-CaMP in brain slices to monitor subcellular calcium signals in dendrites and dendritic spines. This application will allow monitoring of dendritic excitability and synaptic plasticity-inducing signals without need for whole-cell patch recording, which is done one cell at a time and washes out the induction of plasticity.

2.3 Imaging of cerebellar neurons in awake, locomoting mice. We will express VNC-CaMP

and compare its temporal properties with that of GCaMP3 during locomotion and sensory activation. Using head-fixed recording methods that are already in full-time use in my laboratory to study locomotion and eyeblink conditioning, we will image VNC-CaMP in identified cell types of the cerebellum. Our past experience (Sullivan et al. 2005, Ozden et al. 2009, 2012) provides a baseline of information.

2.3a. Cerebellar granule cells. Granule cells (GCs) can be labeled using AAV and the synapsin promoter (**Figure 6**). GCs in lobule IV/V show widespread activation during locomotion and in response to aversive stimuli; signals from consecutive bursts appear to be merged (see Preliminary Results). VNC-CaMP will be used to achieve better temporal resolution and eliminate the possibility of signal saturation. We will test whether VNC-CaMP can track activity in individual parallel fibers (Atluri and Regehr 1996). To test the spike and NMDA-R contribution to GC signals (Gall et al. 2005), cell-attached patch recordings will be done in slices to monitor firing simultaneously with imaging, using APV to separate calcium sources pharmacologically.

2.3b. Molecular layer interneurons. VNC-CaMP will be expressed to probe the dynamics of inhibitory neuron signals. When injected into the cerebellar cortex, AAV containing the synapsin promoter drives expression in molecular layer interneurons with about 10:1 specificity over Purkinje cells (Kuhn et al., 2012). In resting and running mice (Ozden et al. 2012) we have found that stellate/basket interneurons fire at 0-100 Hz, making them an attractive target for VNC-CaMP. In brain slices, patch clamp recording will be done to compare current injection-evoked signals (i.e. signals that arise from spikes only) with signals evoked by parallel fiber stimulation. APV will be used to quantify the contribution of NMDA receptors (Sullivan et al. 2005).

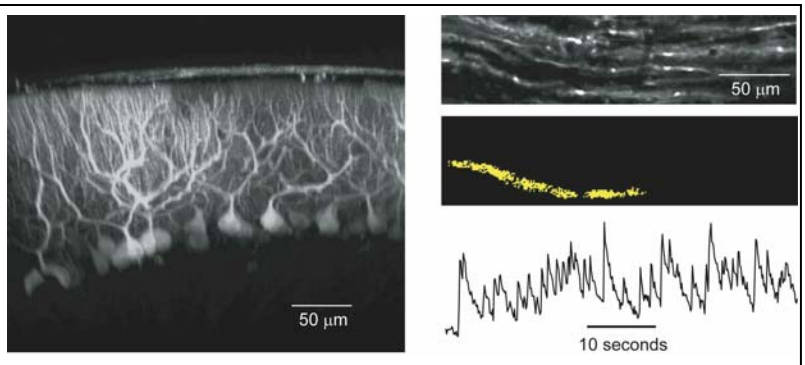

Figure 8: *In vivo* Purkinje cell signals. *Left*, reconstruction of Purkinje cells 16 days after injection of AAV-Tet-D3cpv-WPRE. *Top right*, single section showing Purkinje cell dendrites. Yellow pixels: single monitored dendrite. *Bottom right*, spontaneous calcium transients. Note the overlap in fluorescence signals from consecutive complex spikes.

2.3c. Purkinje cells. Purkinje cells (PCs) generate a rich variety of calcium signals in dendritic spines (Wang et al. 2000; Sarkisov and Wang 2008), dendritic branchlets (Wang et al. 2000, Rancz and Häusser 2006), and the entire dendritic arbor (Tank et al. 1988). These signals extend into the micromolar range (Wang et al. 2000) and regulate excitability and long-term plasticity. Although these mechanisms have been observed in slices, it is not known how they act in waking behavior.

We will address these questions by imaging VNC-CaMP in the PC dendrites of awake, head-fixed animals. The synapsin promoter does not drive PC expression strongly (Kuhn et al., 2012), necessitating a different expression strategy than for GCs or molecular layer interneurons. Two AAVs will be used, one with the human synapsin promoter (hSYN) driving expression of the Tetracycline (Tet) transactivator (tTA) (rAAV_hSYN_tTA) and one with a bidirectional Tet promoter (Tet-bi) driving GECI expression (rAAV_Tet-bi_GECI). This strategy drives specific GECI expression in PCs (**Figure 8**). PC dendrites are clearly separated mediolaterally (**Figure 8**, upper right).

Dendritic climbing fiber-evoked calcium spikes occur in vivo at ~1 Hz (Ozden et al. 2008a,b). OGB-1 measurements show a fast falling phase ($t_{1/2}$ = 0.17 s; Sullivan et al. 2005). GECI off-responses are slower and may limit the resolution of consecutive spikes (**Figure 7** lower right). VNC-CaMP will be used to detect individual complex spikes, as well as identify whether subdendritic signals (Wang et al. 2000, Rancz and Häusser 2006) occur in vivo. VNC-

CaMP will also be tested as a means of monitoring sodium spike rate by imaging the axon initial segment (Palmer et al. 2010).

Alternate approaches and caveats: If brain movement interferes with signal, VNC-CaMP constructs will be made that incorporate mCherry. Since this approach is close to AAV's capacity (4.5 kb, which is enough for two GECIs but borderline for an additional mCherry), an alternate approach is in utero electroporation and imaging in neocortex (Dombeck et al. 2010).

TIMELINE: Objective 1 will begin in Year 1. Objective 1.1, improvements to GCaMP3, will be largely completed by Q4 of Year 1, with improvements continuing into Year 2. Objective 1.2, including virus construction for expressing VNC-CaMP, will be done between Q3 of Year 1 and Q1 of Year 2. Objective 2 will begin in Q4 of Year 1. Objectives 2.1 and 2.2 will start in Q4 of Year 1 and be completed by Q2 of Year 2. Objective 2.3 will be done throughout all of Year 2.

E. SIGNIFICANCE

Compared with the fastest GECI off-response reported, τ=140 ms for TN-XL (Mank et al. 2006), later efforts such as TN-XXL-series indicators, other FRET-based probes such as D3cpv or cameleons, and single-fluorophore probes such as GCaMP3 and GCaMP5 have been 2- to 10-fold slower. Speeding the off-response of GECIs will allow improved tracking of calcium transients. Achieving Virtual Negative Cooperativity by co-expressing multiple variants will furthermore broaden the dynamic range of detectable signals. Here are three examples of experiments that can be addressed using VNC-CaMP.

(1) Firing rate readout in vivo. In neuronal processes, action potential-driven calcium changes rise in ~1 ms and can fall in 15-100 ms (Higley and Sabatini 2008, Hires et al. 2009), opening the possibility of using calcium to resolve individual spike times and changes in firing rate with 1-100 ms resolution. However, calcium changes in small compartments can easily saturate existing GECIs even at moderate firing rates. VNC-CaMP will allow improved tracking of firing rates in vivo. A particularly attractive target is interneurons, which often fire continuously at rates approaching 100 Hz.

(2) Synaptic plasticity signals. In many synapses, long-term potentiation (LTP) and long-term depression (LTD) are both driven by calcium. LTP is thought to require large, brief changes in calcium (1-10 μM for <1 s), whereas LTD putatively requires changes of less than 1 μM lasting for many seconds. These signals are challenging to resolve in vivo without the use of GECIs. Expression of VNC-CaMP will allow plasticity signals to be imaged across populations of synapses with high contrast, an imaging regime that would otherwise require single-cell loading using an electrode, a method that is disruptive to the neuron and surrounding tissue.

(3) Monitoring activity in specific cell types in brain slices and in vivo. The increased availability of cell- and tissue-specific Cre lines (Madisen et al. 2010) from sources such as the Allen Institute for Brain Science and GENSAT allows VNC-CaMPs to be applied to monitoring subcellular, single-cell, and neural circuit activity, both in culture and in intact tissue.

In summary, we anticipate that VNC-CaMPs will become valuable additions to the genetically encodable physiology toolbox. The technology is likely to be at least partly portable to related probes based on CaM and RS20 (GCaMP5, many FRET-based indicators), and will be of use to the entire neuroscience community.

REFERENCES

Akerboom J, Vélez Rivera JD et al. (2009) Crystal structures of the GCaMP calcium sensor reveal the mechanism of fluorescence signal change and aid rational design. ***J Biol Chem*** 284:6455-6464.

Atluri PP, Regehr WG (1996) Calcium transients in cerebellar granule cell presynaptic terminals. ***J Neurosci*** 16:5661-5671.

Bagchi IC, Huang QH, Means AR (1992) Identification of amino acids essential for calmodulin binding and activation of smooth muscle myosin light chain kinase. ***J Biol Chem*** 267:3024-3029.

Black DJ, Tikunova SB et al. (2000) Acid pairs increase the N-terminal Ca2+ affinity of CaM by increasing the rate of Ca2+ association. ***Biochem*** 39:13831-13837.

Brand AH, Perrimon N (1993) Targeted gene expression as a means of altering cell fates and generating dominant phenotypes. ***Development*** 118:401-415.

Chin D et al. (1997) Functional consequences of truncating amino acid side chains located at a calmodulin-peptide interface. ***J Biol Chem*** 272:5510-5513.

Chin D and Means AR (1996) Methionine to glutamine substitutions in the C-terminal domain of calmodulin impair the activation of three protein kinases. ***J Biol Chem*** 271:30465-30471.

Crivici A and Ikura M (1995) Molecular and structural basis of target recognition by calmodulin. ***Annu Rev Biophys Biomol Struct*** 24:85-116.

Doll RF, Crandall JE, Dyer CA, Aucoin JM, Smith FI (1996) Comparison of promoter strengths on gene delivery into mammalian brain cells using AAV vectors. ***Gene Ther*** 3:437-447.

Dombeck DA, Harvey CD, Tian L, Looger LL, Tank DW (2010) Functional imaging of hippocampal place cells at cellular resolution during virtual navigation. ***Nature Neuroscience*** 13:1433-1440.

Donnelly ML, Luke G, Mehrotra A, Li X, Hughes LE, Gani D, Ryan MD (2001) Analysis of the aphthovirus 2A/2B polyprotein 'cleavage' mechanism indicates not a proteolytic reaction, but a novel translational effect: a putative ribosomal 'skip'. ***J Gen Virol*** 82:1013-1025.

Faas GC, Raghavachari S, Lisman JE, Mody I (2011) Calmodulin as a direct detector of Ca2+ signals. ***Nat Neurosci*** 14:301-304.

Gall D, Prestori F, Sola E, D'Errico A, Roussel C, Forti L, Rossi P, D'Angelo E (2005) Intracellular calcium regulation by burst discharge determines bidirectional long-term synaptic plasticity at the cerebellum input stage. ***J Neurosci*** 25:4813-4822.

Granstedt AE, Szpara ML, Kuhn B, Wang SS-H, Enquist LW (2009) Fluorescence-based monitoring of activity in virally traced neural circuits. ***PLoS One*** 9:e6923.

Granstedt AE, Kuhn B, Wang SS-H, Enquist LW (2010) Calcium imaging of neuronal circuits in vivo using a circuit-tracing pseudorabies virus. ***Cold Spring Harbor Protocols*** pdb.prot5410.

Heim N, Griesbeck O (2004) Genetically encoded indicators of cellular calcium dynamics based on troponin C and green fluorescent protein. ***J Biol Chem*** 279:14280-14286.

Hendel T, Mank M, Schnell B, Griesbeck O, Borst A, Reiff DF (2008) Fluorescence changes of genetic calcium indicators and OGB-1 correlated with neural activity and calcium in vivo and in vitro. ***J Neurosci*** 28:7399-7411.

Higley MJ, Sabatini BL (2008) Calcium signaling in dendrites and spines: practical and functional considerations. ***Neuron*** 59:902-913.

Hires SA, Tian L, Looger LL (2009) Reporting neural activity with genetically encoded calcium indicators. ***Brain Cell Biol*** 36:69-86.

Johnson JD, C Snyder, M Walsh, M Flynn (1996) Effects of myosin light chain kinase and peptides on Ca^{2+} exchange with the N-and C-terminal Ca^{2+} binding sites of calmodulin. ***J Biol Chem*** 271:761.

Kuhn B, Ozden I, Lampi Y, Hasan MT, Wang SS-H (2012) An amplified promoter system for targeted cerebellar expression of calcium indicator proteins. ***Frontiers in Neuroscience,*** in review.

Li H, Foss SM, Dobryy YL, Park CK, Hires SA, Shaner NC, Tsien RY, Osborne LC, Voglmaier SM (2011) Concurrent imaging of synaptic vesicle recycling and calcium dynamics. ***Front Mol Neurosci*** 4:34. Epub 2011 Nov 2.

Lin DM, Goodman CS (1994) Ectopic and increased expression of Fasciclin II alters motoneuron growth cone guidance. ***Neuron*** 13:507-523.

Looger LL, Griesbeck O (2011) Genetically encoded neural activity indicators. ***Curr Opin Neurobiol*** 22:18-23.

Madisen L, Zwingman TA, Sunkin SM, Oh SW, Zariwala HA, Gu H, Ng LL, Palmiter RD, Hawrylycz MJ, Jones AR, Lein ES, Zeng H (2010) A robust and high-throughput Cre reporting and characterization system for the whole mouse brain. ***Nat Neurosci*** 13:133-140.

Mainen ZF, Maletic-Savatic M, Shi SH, Hayashi Y, Malinow R, Svoboda K (1999) Two-photon imaging in living brain slices. ***Methods*** 18:231-239, 181.

Mank M, Reiff DF, Heim N, Friedrich MW, Borst A, Griesbeck O (2006) A FRET-based calcium biosensor with fast signal kinetics and high fluorescence change. ***Biophys J*** 90:1790-1796.

Mao T, O'Connor DH, Scheuss V, Nakai J, Svoboda K (2008) Characterization and subcellular targeting of GCaMP-type genetically-encoded calcium indicators. ***PLoS One*** 3:e1796.

Meador WE, Means AR, Quiocho FA (1992) Target enzyme recognition by calmodulin: 2.4 A structure of a calmodulin-peptide complex. ***Science*** 257:1251-1255.

Nakai J, Ohkura M, Imoto K (2001) A high signal-to-noise Ca^{2+} probe composed of a single green fluorescent protein. ***Nat Biotechnol*** 19:137-141.

Ozden I, Sullivan MR, Lee HM, Wang SS-H (2009) Reliable coding emerges from coactivation of climbing fibers in microbands of cerebellar Purkinje neurons. ***Journal of Neuroscience*** 29:10463-10473.

Ozden I, Dombeck DA, Hoogland TM, Tank DW, and Wang SS-H (2012). Widespread state-dependent shifts in cerebellar activity in locomoting mice. ***PLoS ONE***, in review.

Palmer LM, Clark BA, Gründemann J, Roth A, Stuart GJ, Häusser M (2010) Initiation of simple and complex spikes in cerebellar Purkinje cells. ***J Physiol*** 588:1709-1717.

Procyshyn RM and Reid RE (1994) A structure/activity study of calcium affinity and selectivity using a synthetic peptide model of the helix-loop-helix calcium-binding motif. ***J Biol Chem*** 269:1641-1647.

Rancz EA, Häusser M (2006) Dendritic calcium spikes are tunable triggers of cannabinoid release and short-term synaptic plasticity in cerebellar Purkinje neurons. ***J Neurosci*** 26:5428-5437.

Reid RE and Hodges RS (1980) Co-operativity and calcium/magnesium binding to troponin C and muscle calcium binding parvalbumin: an hypothesis. ***J Theor Biol*** 84:401-444.

Sarkisov DV, Wang SS-H (2008) Order-dependent coincidence detection in cerebellar Purkinje neurons at the inositol trisphosphate receptor. ***Journal of Neuroscience*** 28:133-142.

Shouval HZ, Wang SS-H, Wittenberg GM (2010) Spike timing dependent plasticity: a consequence of more fundamental learning rules. Invited review, special issue on spike timing dependent plasticity, ***Frontiers in Neuroscience*** 4:19, ed. H. Markram, P.J. Sjöström, W. Gerstner.

Spradling AC, Rubin GM (1982) Transposition of cloned P elements into Drosophila germ line chromosomes. ***Science*** 218:341-347.

Strynadka NCJ and James MNG (1989) Crystal structures of the helix-loop-helix calcium-binding proteins. ***Annu Rev Biochem*** 58:951-998.

Su Z, Fan D, George SE (1994) Role of domain 3 of calmodulin in activation of calmodulin-stimulated phosphodiesterase and smooth muscle myosin light chain kinase. ***J Biol Chem*** 269:16761.

Sullivan MR, Nimmerjahn A, Sarkisov DV, Helmchen F, and Wang SS-H (2005) In vivo calcium imaging of circuit activity in cerebellar cortex. ***J Neurophysiol*** 94:1635-1643.

Tank DW, Sugimori M, Connor JA, Llinás RR (1988) Spatially resolved calcium dynamics of mammalian Purkinje cells in cerebellar slice. ***Science*** 242:773-777.

Tian L et al. (2009) Imaging neural activity in worms, flies and mice with improved GCaMP calcium indicators. ***Nat Methods*** 6:875-881.

Tsien RY (1999) Monitoring cell calcium. In: *Calcium as a Cellular Regulator* (Ed. E Carafoli and CB Klee) Oxford University Press, pp. 28-54.

Tsien RY (2009) Indicators based on fluorescence resonance energy transfer (FRET). ***Cold Spring Harbor Protocols*** 2009(7):pdb.top57.

Wang SS-H, Denk W, Häusser M (2000) Coincidence detection in single dendritic spines mediated by calcium release. ***Nat Neurosci*** 3:1266-1273.

Weinstein H, Mehler EL (1994) Ca(2+)-binding and structural dynamics in the functions of calmodulin. ***Annu Rev Physiol*** 56:213-236.

Williams RJP (1999) Calcium: the developing role of its chemistry in biological evolution. In *Calcium as a cellular regulator* (Ed. E. Carafoli and C.B. Klee) Oxford University Press, pp. 3-27.

Wu X and Reid RE (1997a) Structure/calcium affinity relationships of site III of calmodulin: testing the acid pair hypothesis using calmodulin mutants. ***Biochem*** 36:8649-8656.

Wu X and Reid RE (1997b) Conservative D133E mutation of calmodulin site IV drastically alters calcium binding and phosphodiesterase regulation. ***Biochem*** 36:3608-3616.

Yang SN, Tang YG, Zucker RS (1999) Selective induction of LTP and LTD by postsynaptic [Ca2+]i elevation. ***J Neurophysiol*** 81:781-787.